



RILEM TC 266-MRP: Round-Robin rheological tests on high performance mortar and concrete with adapted rheology—evaluating structural build-up at rest of mortar and concrete

Sofiane Amziane · Kamal Khayat · Mohammed Sonebi · Arnaud Perrot 

Received: 17 April 2023 / Accepted: 1 September 2023 / Published online: 14 September 2023
© The Author(s), under exclusive licence to RILEM 2023

Abstract This paper presents the results of a round-robin testing program undertaken by RILEM TC-266-Measuring Rheological Properties of Cement-Based Materials in May 2018 at the Université d'Artois in Bethune, France. Seven types of rheometers were compared; they consisted of four ICAR rheometers, Viskomat XL rheometer, eBT-V rheometer, Sliding Pipe Rheometer (SLIPER), RheoCAD rheometer, and 4SCC rheometer, as well as the plate test. This paper discusses the results of the evolution of the static yield

stress at rest of three mortar and five concrete mixtures that were determined using two ICAR rheometers, Viskomat XL, and eBT-V rheometers, as well as the plate test. For the measurements carried out with rheometers, three different structural build-up indices (i.e., structural build-up rate, critical time, and coupled effects of initial static yield stress and rate of structural build-up) were determined. The indices were established using: (i) two static yield stress values measured after 10 and 40 min of rest; and (ii) two static yield stress values measured after 10 and 40 min of rest plus the initial dynamic yield stress (no rest and obtained from the flow curves). The paper discusses the test results and highlights inaccuracies that could be encountered in determining the static yield stress. Test results indicate that the ICAR rheometers and the selected thixotropic indices can provide similar results, and that the spread of results obtained from different rheometers can be considerably reduced when using three yield stress values to calculate the

RILEM TC 266-MRP: Chair: Mohammed Sonebi.

Deputy Chair: Dimitri Feys.

TC Members: Sofiane Amziane, Rolands Cepuritis, Chafika Djelal-Dantec, Khadija El Cheikh, Siamak Fakhryee Nejad, Shirin Fataei, Dimitri Feys, Markus Greim, Steffen Grünewald, Michael Haist, Irina Ivanova, Stefan Jacobsen, Helena Keller, Kamal Khayat, Karel Lesage, Laurent Libessart, Julian Link, Dirk Lowke, Viktor Mechtcherine, Ivan Navarrete, Arnaud Perrot, Tilo Proske, Nicolas Roussel, Wolfram Schmidt, Geert de Schutter, Egor Secrieru, Mohammed Sonebi, Yannick Vanhove, Jon E. Wallevik, Ammar Yahia, Jiang Zhu.

S. Amziane

CNRS, Sigma, Institut Pascal, Université Clermont Auvergne, Clermont-Ferrand, France

K. Khayat

Missouri S&T, Center for Infrastructure Engineering Studies, Rolla, MO, USA

M. Sonebi

School of Natural and Built Environment, Queen's University Belfast, Belfast, Northern Ireland, UK

A. Perrot (✉)

UMR CNRS 6027, IRDL, Univ. Bretagne-Sud, 56100 Lorient, France
e-mail: arnaud.perrot@univ-ubs.fr



rate of the static yield stress at rest. In order to enhance the accuracy of measurements, it is recommended to increase the number of measurements of the yield stress to at least three points over one hour after mixing.

Keywords Dynamic yield stress · Concrete · Mortar · Static yield stress · Thixotropy · Structural build-up

1 Introduction

Fresh cement-based materials undergo microstructural changes due to particles flocculation and formation of early hydration products. This evolution at the microscale induces a strengthening and a rigidification of the material that can interfere with the processing of the fresh material. Such phenomenon, so-called thixotropic behavior, is often described by the increase in the static yield stress of the cementitious material left at rest. Roussel et al. showed in [1, 2] that the rate of increase of static yield stress with resting time is almost constant during the dormant period which depends on the hydration kinetics. Moreover, during shear solicitation, bond between cement particles can be broken, leading to the so-called structural breakdown. In this situation, the cementitious material can partly or totally recover its initial microstructure with a decrease in yield stress which depends on the solicitation duration and on the shear rate [3–5]. At rest, the rate of increase in static yield stress is referred to as structural build-up rate (A_{thix}) [1, 6]. More accurate modelling of the static yield stress increase are developed [7–10], yet the A_{thix} parameter is shown to enable the modeling of the majority of concrete or cementitious materials processing methods, including materials used for additive manufacturing [11, 12]. It is worth noting that the structural build-up of cementitious materials can be reversible as long as a mixing system is able to break the flocculated network and the early hydrate bond [3, 13]. In addition to the rate of structural build-up (A_{thix}) at early stage of hydration, which corresponds to the linear portion of the increase in yield stress with resting time, the static yield stress after a short period of rest (e.g., 15 min) and the coupled effect of this value and A_{thix} have been

proposed as structural build-up indices to evaluate thixotropy [14].

It is worth noting that the chemical activity of the cement is responsible for the structural build-up. However, the addition of sand and gravel in the material can significantly change the strengthening kinetics and thixotropy [15, 16] and makes the experimental measurements more difficult, especially due to the increase in the representative volume of tested materials [17].

In addition to the structural build-up approach, thixotropy can be evaluated by the structural breakdown. Lapasin et al. [18] used the drop in shear stress (τ_i) corresponding to the initial structural condition of the cement-based material and that following shear stress decay to achieve equilibrium (τ_e) to evaluate thixotropy. The test is repeated at different shear rates (e.g., four shear rate values), and the area between the initial flow and equilibrium flow curves “breakdown area (A_b)” can be used to assess thixotropy. The structural breakdown method determined using four shear rate values is shown to closely correspond to the drop in apparent viscosity at a given shear rate, hence facilitating the testing protocol for mortar and concrete [5]. It is important to stress that structural build-up at rest cannot be confused with workability loss, which defines the global strengthening of the cement-based materials even under continuous shearing (e.g., in a concrete mixing truck) [3, 19]. Various workability test methods can be used to evaluate the rate of structural build-up at rest when samples are maintained at rest [14, 20, 21].

Proper assessment of the structural build-up of the cementitious materials is crucial for modern concrete processing to enhance productivity in the concrete construction market. It is advantageous to increase the structural build-up with resting time in casting of self-consolidating concrete (SCC) to reduce lateral pressure exerted on the formwork [8, 22–27]. For high casting rates, hydrostatic pressure profile can occur; however, the lateral pressure can significantly decrease with the reduction of the casting rate and the increase in concrete thixotropy; the lateral pressure is closely correlated to the ratio $A_{\text{thix}}/\text{casting rate}$. The increase in structural build-up at rest can also enhance the stability of the mixture [28, 29]. Structural build-up is also involved in other processing issues, such as distinct layer casting [30–32].



More recently, the structural build-up rate has been shown to limit the printing rate in the additive manufacturing process of cementitious materials [11, 12, 33–35]: the base layer must have sufficient strength to sustain the weight of subsequent deposited layers. The modeling of the failure of the base layer can then be described using the ratio of the structural build-up rate to the printing rate (i.e., speed of printing) [35, 36].

The determination of the structural build-up rate is based on the measurement of the static yield stress of the material and its variation with resting time. This can be done on different samples using invasive tests [20, 37], such as the portable vane test or undisturbed slump flow test (for SCC), or non-invasive tests, such as the plate test that allows continuous assessment of the static yield stress on the same test sample [38]. Other types of non-destructive tests, such as ultrasonic measurement can be employed to assess the increase in static yield stress [39]. More recently, the single sample strategy, which consists of carrying the test on the same sample, has been shown to provide results that are similar to the multiple sample approach of testing undisturbed samples [40–43]. For example, when evaluating the increase rate of static yield stress at rest of fresh cement paste and mortar by performing vane test measurements at 20-min intervals during 80 min, Ivanova and Mechtcherine [40, 41] showed that the difference of results between a multiple-batch procedure and a single-batch approach can be limited to approximately 10%. The former approach consists in reaching the critical strain to minimize the breakdown effect and limit the effect of the tests on the built-up microstructure of the tested material.

Despite the numerous attempts in assessing the static yield stress of cement-based materials, there is a need to recommend a testing procedure to evaluate the structural build-up of cement-based materials, especially at the mortar and concrete scales. To advance toward a standardized procedure, it is necessary to evaluate measurement variability for the different test methods and estimate measurement reliability when the same test is determined using multiple instruments.

The aim of the study is to assess the structural build-up rate at rest of concrete and mortar mixtures using data obtained during the TC 266-MRP Round Robin Test. The testing program involved the comparison of several rheological testing equipment, including those used to assess dynamic and static yield stresses,

interfacial rheometry, and workability tests. Measuring static yield stress, which is reported in this paper, involved the use of two ICAR rheometers, Viskomat XL rheometer, eBT-V rheometer, RheoCAD rheometer, and the plate test. The static yield stress of three mortar mixtures and five concrete mixtures was determined. The investigation during the Round Robin Test on static yield stress had three major objectives:

- (1) Evaluate the structural build-up indices to capture the stiffening effect and compare measurements that can be obtained from different devices;
- (2) Determine the accuracy of determining thixotropy indices using two and three data points;
- (3) Provide guidance and recommendations to evaluate the structural build-up of mortar and concrete.

2 Physical background on yield stress measurements

2.1 Static and dynamic yield stress

With resting time, the increasing shear stress necessary to make the material flow, which is related to the state of structuration of cement particles assembly, is called static yield stress, $\tau_{0,s}$. Static yield stress is significantly higher than the dynamic yield stress, $\tau_{0,d}$, which is related to the non-structured cementitious material network. It is important to note that the static yield stress of a material not subjected to a resting time can be considered to be equal to the dynamic yield stress. Reflecting the non-structured cement particles suspension [2].

When considering the rheological behavior of cementitious materials, it is important to distinguish between the steady state and transient/time-dependent properties [6]. The steady-state rheological behavior of cementitious materials corresponds to the rheological behavior of the materials at the unstructured state (i.e., the state of non-flocculated cement particles: assembly with no nucleation points). As shown in [17], those properties are measured after adequate pre-shearing of the materials to completely disperse any flocculated cement grains and reduce friction in the granular skeleton on the mortar and concrete scales [16, 44–46].

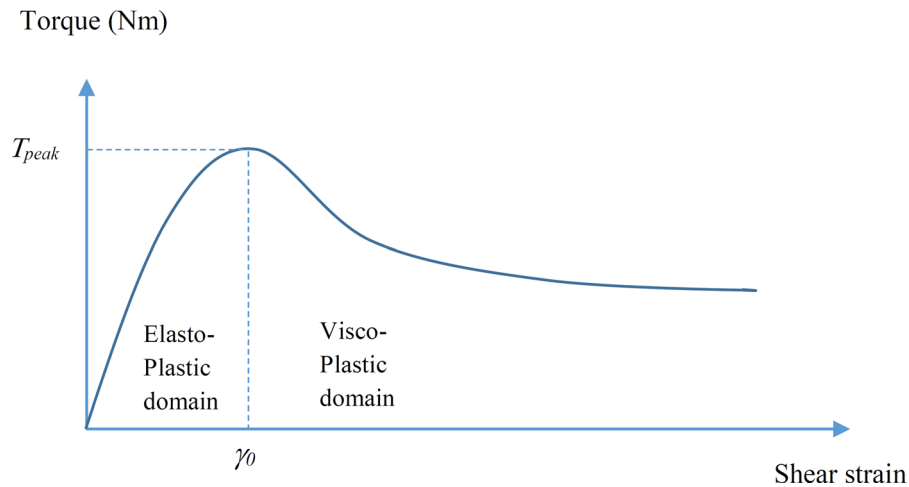


Fig. 1 Example of stress growth test results. The shear strain of the x-axis is the product of the testing time by the constant shear rate

On the contrary, at rest or at a very low strain rate, the cement particles network can build-up, and internal friction between aggregate particles for mortar and concrete is amplified [16]. Such structural build-up is commonly known as thixotropic behavior of cementitious materials induced by flocculation (during few minutes), cement particles nucleation at the contact point (during dozens of minutes), as well as internal friction of the granular skeleton (sand and coarse aggregate). This build-up of the microstructure is reversible at the plastic state when the mixing and processing can induce sufficient shear rate to prevent/reverse the restructuring of the system [3, 13]. The breakage of bond among cement particles and friction among aggregate particles is referred to as structural breakdown. It is important to note that part of the static yield stress increase due to thixotropic behavior corresponds to the reversible part of the increase of shear stress that is captured by comparing structural build-up and breakdown.

After a short period of rest (e.g., 20 min), the static yield stress can evolve linearly with resting time [4, 5], although more elaborate models can offer a more accurate description of the time evolution of the static yield stress when the rate of increase in static yield stress is no longer linear. For example, a double timescale model can be used to differentiate the nucleation and flocculation mechanisms [9, 10, 47], and an exponential model can be relevant when in systems with accelerated structural build-up [7]. The

linear model of static yield stress increase can be expressed as follows (Eq. 1):

$$\tau_{0,s}(t) = \tau_{0,s}(0) + A_{mix}t \quad (1)$$

where t is the resting time. The static yield stress is commonly measured using the so-called stress growth procedure [37, 48, 49]. This method uses vane or coaxial cylinders geometry and consists in applying a constant and sufficiently low shear rate (values reported in the literature vary between 5×10^{-4} and 10^{-2} s^{-1} , depending on the cementitious materials) to make the viscous effects negligible. It is important to note that the applied strain must be sufficient to actually yield the material, as pointed out by Nerella et al. [43]. When the torque peak, T_{peak} , is recorded (sufficient strain reached), as shown in Fig. 1, the yield stress can be computed from a simple stress balance on the sheared surface (Eq. 2):

$$\tau_{0,s} = \frac{T_{peak}}{2\pi r^2 (h + i \frac{r}{3})} \quad (2)$$

where i is an integer value, which can be 0, 1, or 2 depending on the shearing conditions at the top and bottom sides of the shear vane or cylinder, and r and h are the radius and height of the sheared surface, respectively. For instance, if the cementitious material is sheared above and under the rotating tool, “ i ” would be equal to 2 (immersed tool). For a slender vane or cylinder, “ i ” can be taken as 0.

Stress growth tests should be performed on undisturbed samples left at rest during the targeted duration.

However, recent studies have shown that the stress growth procedure can be carried out on the same sample without considerably altering the measured yield stress (around 10% variation of shear stress from values determined on undisturbed samples) [40]. Such methods using a single sample, if less accurate, can be used to save materials and testing time [40, 43, 50]. Other methods can be used to determine static yield stress, such as linear increasing stress sweep [51] and material creep recovery test [52–54].

2.2 Structural build-up or thixotropy indices from yield stress evolution

Several thixotropic indices can be used to determine the degree of structural build-up at rest. In addition to the rate of structural build-up at rest (A_{thix}), the characteristic time (t_c) corresponding to the ratio between the initial yield stress and the structural build-up rate (A_{thix}) is equal to the time required to double the initial yield stress value. Also, the product of the structural build-up rate with the static yield stress value after a relatively short resting period (e.g., 15 min) has been shown to be efficient to account for the combined effect of initial structural build-up at rest (i.e., reflecting initial flocculation) and the rate of structural build-up at rest over an extended rest period [60].

3 Methodology

3.1 Materials and devices

This work is part of the round-robin test carried out by RILEM TC 266-MRP at the Université d'Artois in Bethune, France in May 2018. It follows 2000's first international benchmark on rheological measurements carried out on mortar and concrete at Nantes [55] and Cleveland [56]. However, almost 20 years later, concrete types have evolved following further development in admixture design in order to make more flowable concrete, including SCC for which structural build-up plays a more important role [15].

Five concrete and three mortar mixtures were evaluated in the round-robin testing campaign. The details of the mixture proportioning as well as the results of the empirical tests are provided in [17]. All mixtures were produced by a commercial ready-mix plant. Once the concrete trucks arrived at the

laboratory, the workability was verified, and adjustments by means of chemical admixtures were performed, if necessary.

The various devices employed during the round-robin testing campaign and for the evaluation of the structural build-up at rest are described in [17]. Five different rheometers with similar geometries and sample volumes and the plate test were used in the round-robin testing program to describe the structural build-up rate. Specific details of these devices are as follows:

- Two four-bladed vane ICAR rheometers with a vane radius of 63.5 mm and height of 127 mm were used for the structural build-up measurements [57]. The rheometers are denoted ICAR 1 and ICAR 2. Using two identical devices allows the evaluation of measurement variations using the same commercial device.
- Couette-type Viskomat XL equipped with a six-bladed vane with a vane radius of 34.5 mm and height of 69 mm.
- The eBT-V rheometer having a six-bladed vane with a vane radius of 51.5 mm and height of 103 mm.
- Rheocad rheometer with a four-bladed vane with vane radius of 60 mm and height of 250 mm.

The rheometers were used to perform static yield stress measurements in addition to flow curve measurements provided in [58]. The precise testing protocol provided for flow curve determination is provided in [17, 58]; the test consisted of pre-shearing the material and imposing a stepwise decreasing rotational velocity profile. Each stepwise profile consisted of eight rotational velocity steps with 5-s duration each. The Reiner-Riwlin equations were used for the transformation of the bulk torque-rotational velocity to shear-stress data [44].

The plate test method was also used to determine the variations of the structural build-up over time. The plate test consists of measuring the mass variation with time of a rough plate or cylinder suspended in a freshly mixed cement paste [59], mortar [38, 59–61] and even concrete [25]. The mass variation allows to compute the evolution of the static yield stress of cement-based materials with time using a simple force balance equation, as detailed in [17]. Such a test is similar to the moving plate test [62], the Lombardi plate cohesion test [63], and the inclined plate test even, if

this last test does not provide a continuous measurement of static yield stress [64].

It is important to note that only the variation of static yield stress was computed using the plate test device because of uncertainty on the initial value. In this case, the structural build-up was computed using Eq. (3):

$$A_{thix} = \frac{g\Delta(\Delta m_{plate}(t))}{S_{plate}\Delta t_{rest}} \quad (3)$$

where g is the gravity acceleration, Δm_{plate} is the recorded mass variation, S_{plate} is the plate surface area immersed in the mortar sample, and Δt_{rest} is the resting time of the sample.

For the round-robin test, the tool was submerged in a mortar or concrete sample cast into a 1.5-m high and 200-mm diameter column; the test necessitates a sample of 45 L. A ribbed steel rebar with a diameter of 15 mm and a length of 130 mm was selected for concrete testing, and a screw with a diameter of 14 mm and a length of 80 mm was employed for the mortar samples. This enabled the adjustment of the roughness of the submerged tool to the particle size of the aggregate of the test sample.

3.2 Measuring procedures and data analysis

3.2.1 Measuring sequence and test procedure

Five wheelbarrows were sampled from ready-mix trucks for rheological and workability testing. For each mixture, the test started ($t = 0$ min) when the concrete was secured from the concrete truck mixer. Flow curve measurement was conducted with each rheometer. At 5 min, the plate test was started. After 10 min, a static yield stress measurement was carried out with each rheometer. The concrete sample was kept in the rheometer buckets at rest for another 30 min. Considering the single batch approach, a second static yield stress measurement was carried out after a resting time of 40 min. Figure 2 summarizes this sequence of measurements that combines the variations of static yield stress estimated with the plate test and the two static yield stress values measured after resting times of 10 and 40 min. The initial dynamic yield stress derived from the flow curve is considered equivalent to the initial static yield stress of an undisturbed sample (i.e., without any resting time).

The dynamic yield stress is measured after a decreasing shear rate ramp that is considered to completely break the reversible bonds between cement grains [13]. The stress value obtained at the minimal shear rate tested during the flow curve measurement is similar to the value computed from the flow curve analysis and is obtained at a similar strain rate. An additional flow curve analysis was carried after 50 min and was shown to provide similar dynamic yield stress values than analysis carried out after the initial ones. This observation supports the ability of the flow curve protocol to reset the microstructure of the tested materials and to provide the initial static yield stress value.

Before each measuring sequence, a calibration step for measurement of static yield stress at rest (carried out without a physical sample) was performed using the following procedure:

- Plot variations in torque (T) as a function of time at constant low rotational velocity of 0.025 rps (N) to check whether the data have been properly recorded from the raw data file for each test sample.
- Average all raw data during the measurement time at constant rotational velocity.
- Verify whether the torque remains constant (or if peak value of T is attained). Report oscillation of the data or any large variations in T vs. N values.
- Report the average torque (in Nm) and average rotational velocity (in rps). This value can help to correct the data collected in a measuring sequence to take into account any offset in the torque.

3.2.2 Analysis of static yield stress measurements

Using rheometers, the static yield stress measurements were performed with the stress growth protocol, as presented in Sect. 2.1. The rotational velocity of the tool was 0.025 rps for ICARs, 0.027 rps for Viskomat XL and 0.034 rps for eBT-V that was applied for 60 s to have sufficient strain to shear the sample. Then, the rotational velocity (N) and torque (T) were plotted as a function of time to verify whether the data had been recorded properly from the raw data file. All torque values were corrected by the initial torque value obtained from the calibration step (T_{corr} : corrected torque values). The static yield stress was computed using Eq. (2) considering that $i = 0$ (in order to make



Rheometer tests: Static yield stress measurements

*Flow curve: Dynamic yield stress
= static yield stress with no rest
**Single batch approach

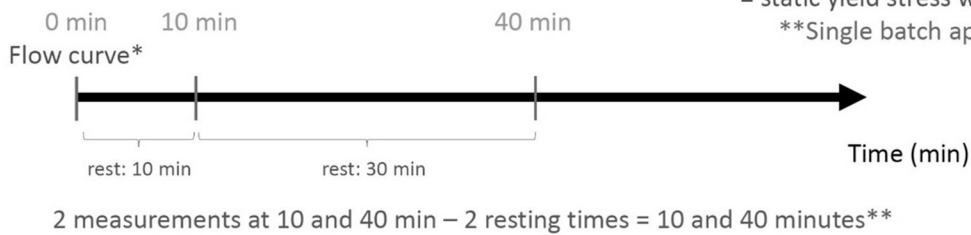


Plate tests

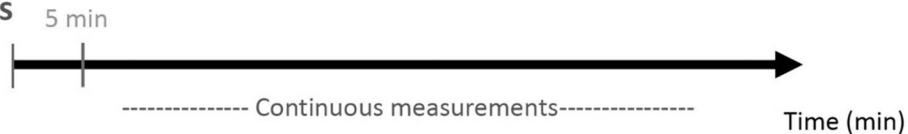


Fig. 2 Summary of static yield stress measuring sequences of the various devices

it consistent with the dynamic yield stress determination using the Reiner-Riwlin approach [44]), which can be written as:

$$\tau_{0,s} = T_{\text{corr-max}} / 2 \pi R_i^2 h \quad (4)$$

As discussed later, all curves were examined to check if they present the expected profile (as shown in Fig. 1), and that no measuring artifact has occurred.

For the plate test, the plate was immersed in the testing material at $t = 5$ min. The length of the immersed part of the plate was measured to compute V_{plate} and S_{plate} . The measurement was stopped at 45 min. Equation (4) was used to compute the evolution of static yield stress with time.

3.2.3 Structural build-up indices

Three structural build-up indices were determined from the various test methods, as follows:

- The structural build-up rate, A_{thix} .
- The critical time to double the initial yield stress value, $t_c = \tau_{0,s0} / A_{\text{thix}}$ (time when $\tau_{0,s}(t_c) = 2\tau_{0,s0}$ introduced in Eq. (4).
- The coupled effect of static yield stress at 10 min of rest and A_{thix} . This index is equal to $C = \tau_{0,s10} \cdot A_{\text{thix}}$.

For A_{thix} , the three thixotropic indices were computed using two different datasets. The first one considered the actual static yield stress measurements carried out after 10 and 40 min of rest. In this case, the

structural build-up rate, $A_{\text{thix}(10-40 \text{ min})}$, can be expressed as (Eq. 5):

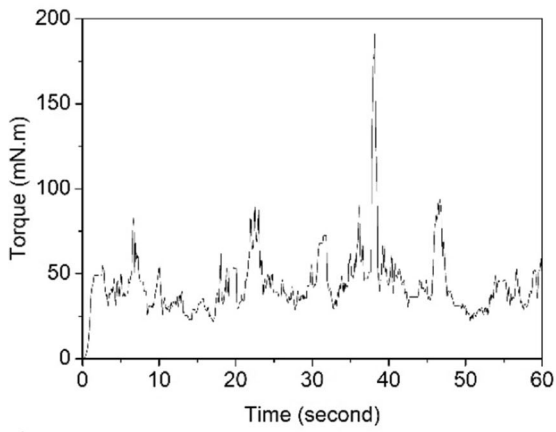
$$A_{\text{thix}(10-40 \text{ min})} = (\tau_{0,s40} - \tau_{0,s10}) / 30 (\text{Pa/min}) \quad (5)$$

The second approach involved estimating $A_{\text{thix}(0-40 \text{ min})}$ based on the best linear interpolation of the static yield stress evolution using three values: rest times of 0 min (corresponding to the dynamic yield stress) in addition to the 10- and 40-min static yield stress values. Note that in this study, the static yield stress evolution over 40 min is considered to be linear given the thixotropic level of the tested mortar and concrete mixtures. The t_c and the coupled effect thixotropic indices were determined using A_{thix} values computed using the second approach of data treatment involving three data points, which provided more reliable results, as discussed below.

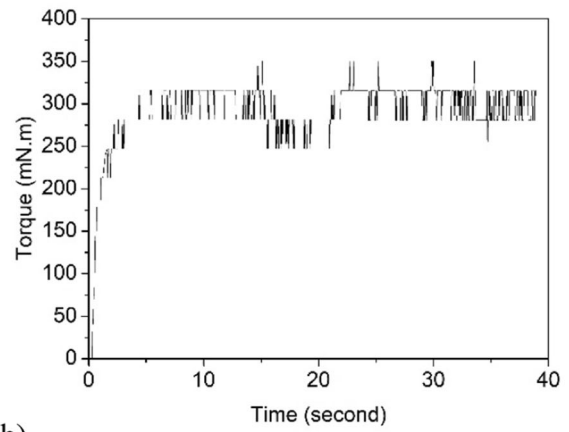
4 Results and discussion

4.1 Static yield stress

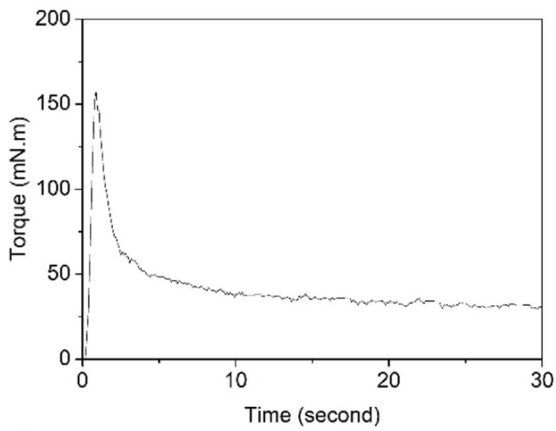
The static yield stress was determined at the maximum torque, which was not clearly obtained in some mixtures. Figure 3 shows the stress growth diagrams of the concrete C2 at 10 min and mortar M2 determined at 40 and 10 min, respectively, that were tested using the Viscomat XL and ICAR1 rheometers, respectively. Indeed, the stress growth diagram showed more fluctuation in measurements for the concrete mixtures (Fig. 3a and b) in comparison to the



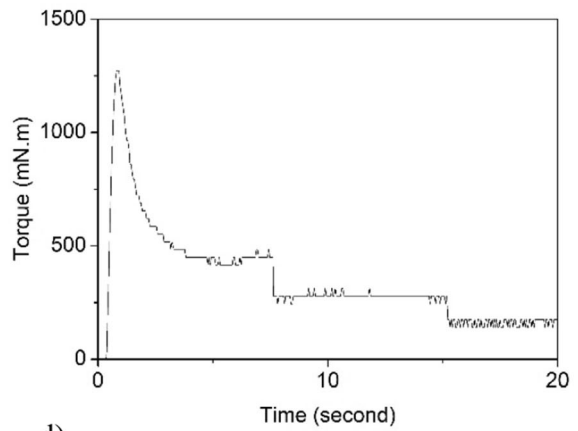
a)



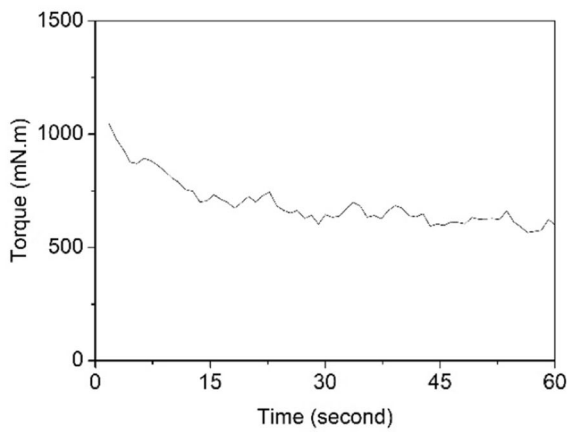
b)



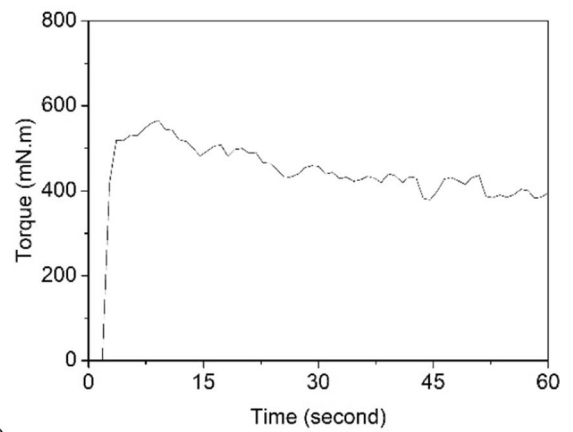
c)



d)



e)



f)



◀ **Fig. 3** (a) Stress growth diagram for Concrete C2 at 10 min with Viscomat XL, (b) stress growth diagram for Concrete C2 at 10 min with ICAR 1, (c) stress growth diagram for Mortar M2 at 40 min with Viscomat XL, (d) stress growth diagram for Mortar M2 at 10 min with ICAR1, (e) stress growth diagram for Concrete C1 at 10 min with RheoCAD, and (f) Stress growth diagram for Concrete C2 at 10 min with RheoCAD

mortar mixtures (Fig. 3c and d). The fluctuation was more pronounced for the concrete sample with coarse aggregate. The significant fluctuation of torque can be observed due to their sensitivity to flow induced segregation related to the larger particle size and relatively low yield stress/viscosity value.

The first value recorded by the RheoCAD was the maximum one, indicating that shearing of the material had already occurred prior to the first measurement. This can lead to an underestimation of the static yield stress when the initial maximum torque value is used for data interpretation. This was the case of the C1 mixture shown in Fig. 3e; the real value of static yield stress cannot be computed from the data contrarily to the C2 mixture in Fig. 3f where the peak torque was clearly attained during the stress growth test.

The static yield stress was calculated using Eq. 4 that assumes that the material is sheared following a cylindrical surface described by the height vertical rotation of the edge of the vane device. This means that the contribution of the lower surface formed underneath the vane cylindrical body is not considered in the yield stress calculation. Moreover, the greater the number of blades used in each rheometer, the more this assumption can be valid. This induces a certain discrepancy for the rheometers with four blades and can explain the higher values of torque obtained with the 4-blade vane tools (ICAR rheometer) compared to the 6-blade vane devices (Viscomat XL and eBT-V rheometers). For example, for the concrete 5, the static yield stress values were 75% on the average higher for the 4-blade vane rheometers than for the 6-blade ones.

4.2 A_{thix} thixotropic index

In order to compare the data obtained from the round-robin test, the A_{thix} values are plotted versus average values of A_{thix} for each of the investigated mixtures. The average results were computed using values obtained with the different rheometers for the same mixture. The methodology of baseline value

computation used in [17] was not been chosen here because of the lower numbers of data points available for each mixture: in the present case, each rheometer has the same weight. The data were analysed using A_{thix} derived from the two static yield stress measurements carried out after 10 and 40 min (Fig. 4a) and also from the three measurements: two static yield stress measurements carried out after 10 and 40 min and the dynamic yield stress value at 0 min (Fig. 4b).

The results for concrete and mortar mixtures showed a relatively large spread (Fig. 4a) with the two-value computation that is reduced when using the three-point analysis for to determine A_{thix} (Fig. 4b). In Fig. 5, the linear fit parameters are found to be in the range of 1.49 for the ICAR1 to 0.63 for the eBT-V. It can be also noted that the R^2 coefficient for the plate test was equal 0.16, which reflects a poor correlation with other measurements. This can be attributed to the fact that the measurement was carried out at the top of a high column sample (more than 1 m) that is sensitive to bleeding and surface settlement.

The measurements of yield stress obtained from the mortar mixtures only are shown in Fig. 5a and b. Compared to the $A_{thix(10-40 \text{ min})}$ values with the linear fit coefficients ranging from 0.45 to 1.27, the computation of the $A_{thix(0-40 \text{ min})}$ values allows a noticeable reduction in the dispersion of structural build-up data with a closer linear fit coefficient of 0.86 to 1.20.

The various fitting parameters reported in Figs. 4, 5, 6 are summarized in Table 1. This reflects the need to increase the number of static yield stress measurements at different resting times to improve the accuracy of the A_{thix} evaluation, as reported in the literature where typically four data points are used to determine A_{thix} [12, 22, 25, 37].

It is interesting to distinguish measurements carried out on mortar and concrete using the 2- and 3-points computational approaches shown in Fig. 5a and b, respectively, and Fig. 6a and b, respectively. For both types of material, using the three values to determine yield stress can reduce data dispersion. For the mortar mixtures, the linear fit coefficients ranged between 0.45 and 1.27 with the two yield stress values measured at 10 and 40 min; these values were 0.86 to 1.2 when the dynamic yield stress was considered in the data analysis.

In the case of concrete, a similar trend was observed, but the A_{thix} values were more dispersed with linear fit coefficients of 0.72 to 1.69 with the 2-point computational approach and 0.73 to 1.48 for



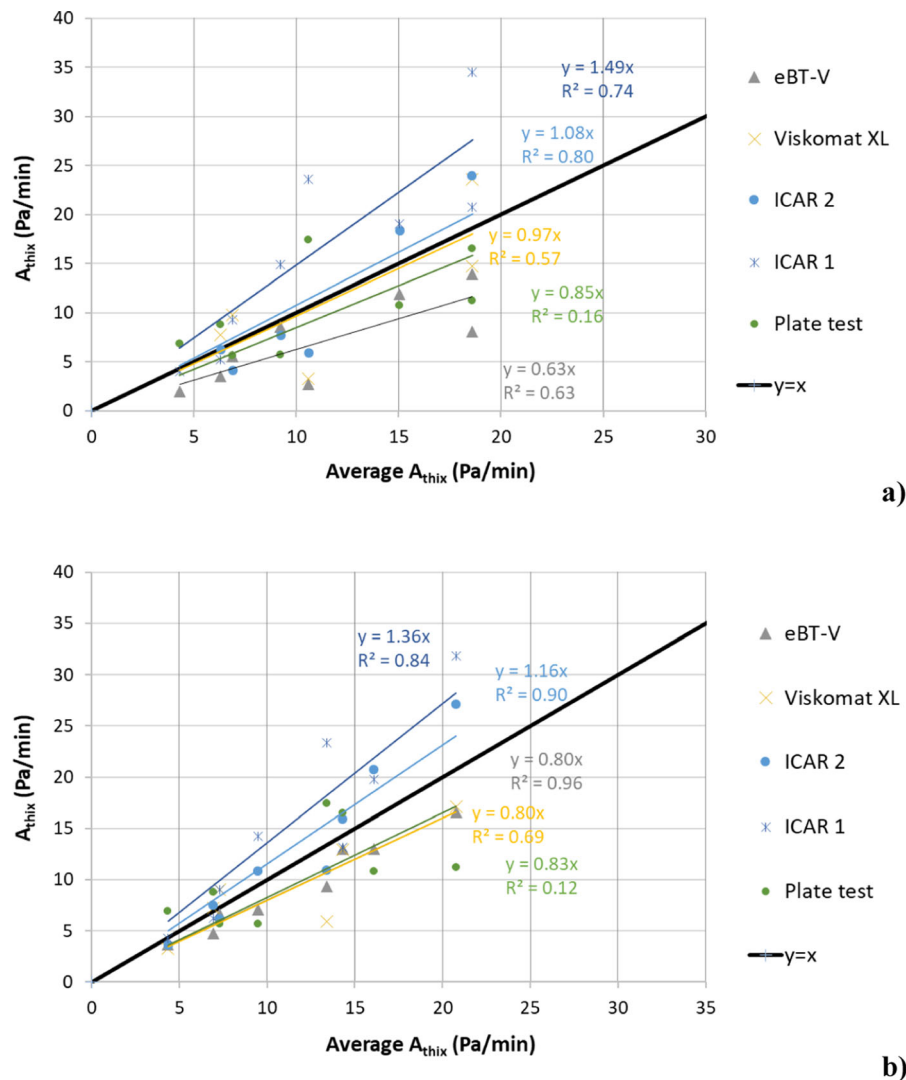


Fig. 4 Measured A_{thix} obtained with (a) static yield stress measurements at 10 and 40 min (two values) in function of the average A_{thix} values computed for each tested material, and (b) static yield stress measurements at 10 and 40 min and

the 3-point approach. For the mortar testing, R^2 values of 0.93–1.00 were obtained with the 3-point computational approach compared to values ranging from 0.19 to 0.97 for the concrete (note that the minimal value of 0.19 was obtained for the plate test). Measuring concrete rheological properties is shown to be more difficult than measuring mortar rheological properties because of the greater levels of granular friction effect and shear-induced particle migration. The ability of the plate test to accurately measure the structuration rate of concrete can be hindered by bleeding (modified water to cement ratio where the

dynamic yield stress measurements (three values) in function of the average A_{thix} values computed for each tested material. Linear fits of the measurements are plotted for each rheometer

plate is immersed) or wall slip (if the plate roughness is not adapted top to the gravel size) at the interface between plate and concrete sample.

Comparing the different rheometers, it is interesting to note that the ranking between the values of A_{thix} obtained by each rheometer (which can be studied using the slope of each regression line), is the same as the one obtained for the dynamic yield stress obtained in [17]. It seems that the initial calibration of the torque sensor plays a major role in the measured A_{thix} value and that it can explain the discrepancy between values.

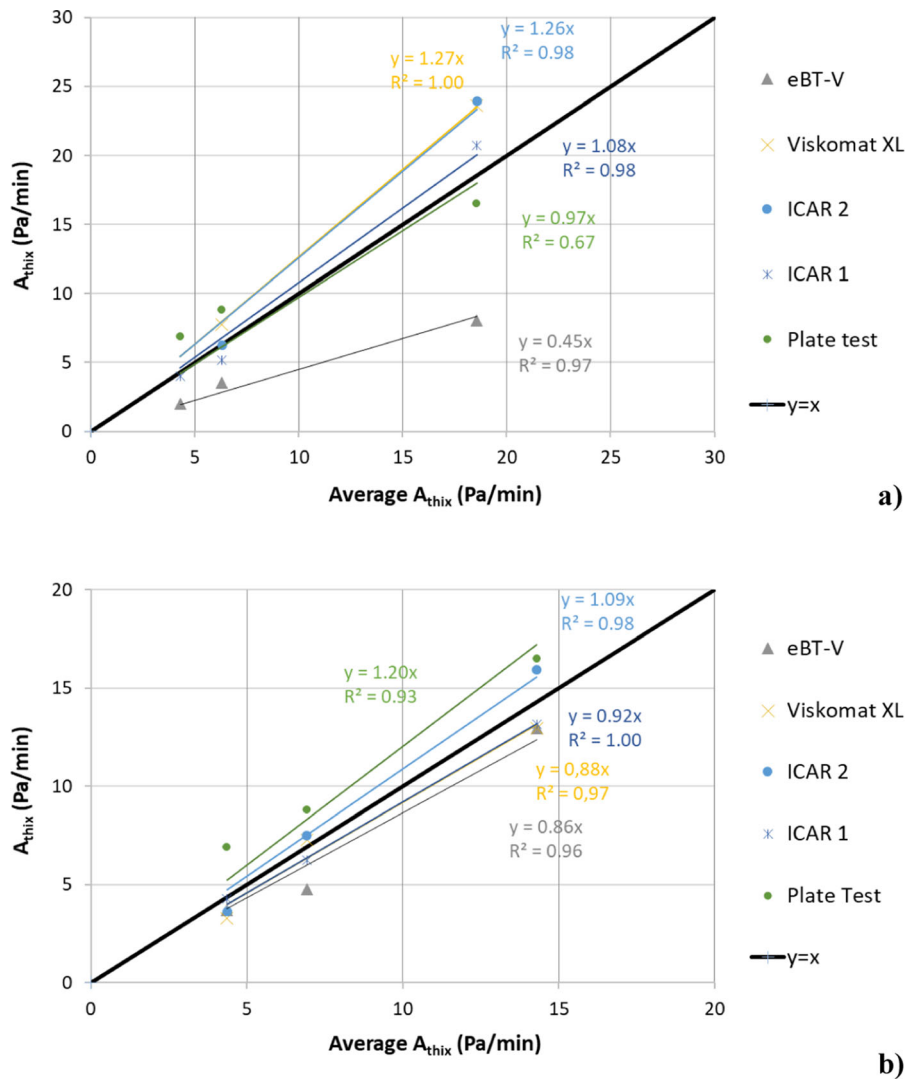


Fig. 5 Measured A_{thix} obtained with (a) static yield stress measurements at 10 and 40 min (two values) vs. average A_{thix} values for each mortar, and (b) static yield stress measurements

at 10 and 40 min and dynamic yield stress (three values) vs. average A_{thix} values for each mortar

4.3 t_c thixotropic index

In order to compare all data obtained from the round-robin test campaign, computed t_c values are plotted versus the average values of t_c for each tested material. The average values were computed using the results obtained with the different rheometers for the same mixture. The data were analysed using t_c that was derived from the static yield stress measurements carried out at 10 and 40 min (Fig. 7a) and the dynamic yield stress value (Fig. 7b). It can be noted that the

plate tests cannot be used in this case because the initial yield stress was not measured using the plate test device. Moreover, one has to keep in mind that results between two and three points are different because they are computed using the 10-min static yield stress for the two points computation and the dynamic yield stress, which is assumed to be the initial static yield stress for the three points computation.

In Fig. 7a, it can be seen that all t_c values are dispersed around the computed average values for each mixture. The comparison of the linear fit



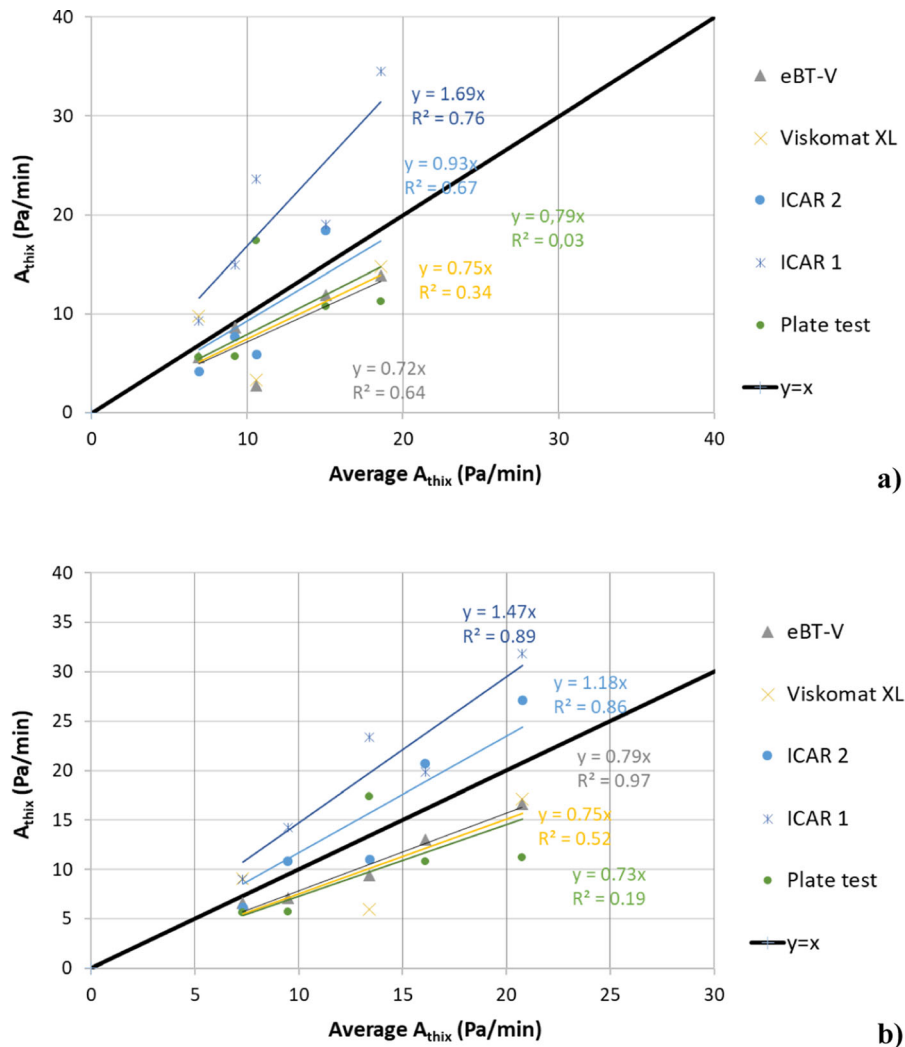


Fig. 6 Measured A_{thix} obtained with (a) static yield stress measurements at 10 and 40 min (two values) vs. average A_{thix} values computed for each concrete, and (b) static yield stress

measurements at 10 and 40 min and dynamic yield stress (three values) vs. average A_{thix} values computed for each concrete

parameter shows that the ICAR 1 rheometer provided the shortest t_c (coefficient equal to 0.35), and the eBT-V rheometer provided the highest t_c (coefficient equal to 1.8). The ranking of rheometers is opposite to the one obtained with A_{thix} . Other devices provided values that are close to the average line (0.83 for the Viskomat XL rheometer and 0.97 for the ICAR 2 rheometer). It can be also noted that the R^2 for the ICAR 1 rheometer was 0.62, which reflects a poor correlation with other measurements.

The comparison of Fig. 7a and b shows that the computation of the t_c values determined using the three yield stress values, instead of two values, reduces

noticeably the dispersion of the measured critical time. As a result, the critical time is shorter for the 3-point computation method. Using a 2-point computational approach leads to a linear fit coefficient ranging from 0.35 to 1.8, while the 3-point approach reduces this range to 0.89 and 1.14. Moreover, the R^2 coefficient for each rheometer is increased when using the three yield stress values, as summarized in Table 1. Therefore, it is important to increase the number of static yield stress measurements at different resting times to improve the accuracy of the t_c evaluation.

Moreover, comparing A_{thix} results with the t_c analysis, it can be seen that the dispersion of the



Table 1 Slope of computed structural build-up indices vs. average values for concrete and mortar

3 points computation–0, 10 and 40 min		ICAR 1		ICAR 2		Plate Test		Viskomat XL		eBT-V	
		Slope	R^2	Slope	R^2	Slope	R^2	Slope	R^2	Slope	R^2
A_{thix}	All	1.36	0.84	1.16	0.9	0.83	0.12	0.8	0.69	0.8	0.96
	Mortar	0.92	1	1.09	0.98	1.2	0.93	0.88	0.97	0.86	0.96
	Concrete	1.47	0.89	1.18	0.86	0.73	0.19	0.75	0.52	0.79	0.96
t_c	All	0.89	0.27	0.98	0.83			0.99	0.81	1.14	0.65
	Mortar	1.28	0.97	0.95	0.68			0.82	0.76	0.95	0.95
	Concrete	0.65	0.38	1	0.92			1.15	0.9	1.26	0.7
$t_c \cdot A_{thix}$	All	1.24	0.82	1.11	0.91			0.62	0.8	0.91	0.69
	Mortar	0.75	0.98	0.95	0.97			0.74	0.99	1.56	0.98
	Concrete	1.34	0.84	1.15	0.86			0.58	1	0.77	0.84
2 points computation–10 and 40 min		ICAR 1		ICAR 2		Plate Test		Viskomat XL		eBT-V	
		Slope	R^2	Slope	R^2	Slope	R^2	Slope	R^2	Slope	R^2
A_{thix}	All	1.49	0.74	1.08	0.8	0.83	0.12	0.97	0.57	0.63	0.63
	Mortar	1.08	0.98	1.26	0.98	0.93	0.67	1.27	1	0.45	0.97
	Concrete	1.69	0.76	0.93	0.67	0.79	0.03	0.75	0.34	0.72	0.64
t_c	All	0.35	-1.62	0.97	0.59			0.83	0.9	1.8	0.88
	Mortar	0.62	0.42	0.76	0.03			0.48	0.09	1.71	0.16
	Concrete	0.26	0.87	1.01	0.47			0.89	0.95	1.83	0.92
$t_c \cdot A_{thix}$	All	1.36	0.71	1.16	0.93			0.78	0.7	0.69	0.9
	Mortar	0.95	1	1.15	1			1.1	1	0.8	1
	Concrete	1.52	0.65	1.17	0.88			0.57	1	0.64	0.84

structural build-up index is reduced when using t_c because of the observed decreased range linear fit coefficients obtained with the critical time. This can be explained by the fact that the computation of the critical time requires to divide A_{thix} by the first yield stress values, which allows to delete the differences in the torque sensor calibration between rheometers. During the whole round-robin experimental campaign, it was observed that ICAR1 quasi-systematically provides a higher yield stress value than the other rheometers that can be attributed to a slightly different sensitivity. The computation of the critical time deletes the calibration and differences (shapes of the device, computation of the yield stress, etc.) between the rheometers and reduces the dispersion between test results.

In order to further analyse the data, it is interesting to distinguish measurements carried out on mortar mixtures using the 2- and 3-points computations, as reported in Table 1, and for the concrete mixtures for

the 2- and 3-points computations. It can be seen that for both mortar and concrete, using three yield stress values helps to reduce the dispersion of the measurements. For the mortar mixtures, the linear fit coefficients ranged between 0.48 and 1.78 with two yield stress values measured at 10 and 40 min; such coefficients were 0.82 to 1.28 when the dynamic yield stress values were considered. For the concrete, the same trend was observed, but the t_c values were more dispersed, as shown by the linear fit coefficients (0.72 to 1.69 using the 2-points computation and 0.65 to 1.26 when the 3-point computation was considered). It is also worth noting that mortar mixtures exhibited higher R^2 values (between 0.68 and 0.97 with the 3-point computation approach). Contrarily, the R^2 coefficient obtained for concrete were lower (between 0.38 and 0.92 for the rotational rheometer). This clearly shows that measuring concrete rheological properties is more difficult than that for the mortar



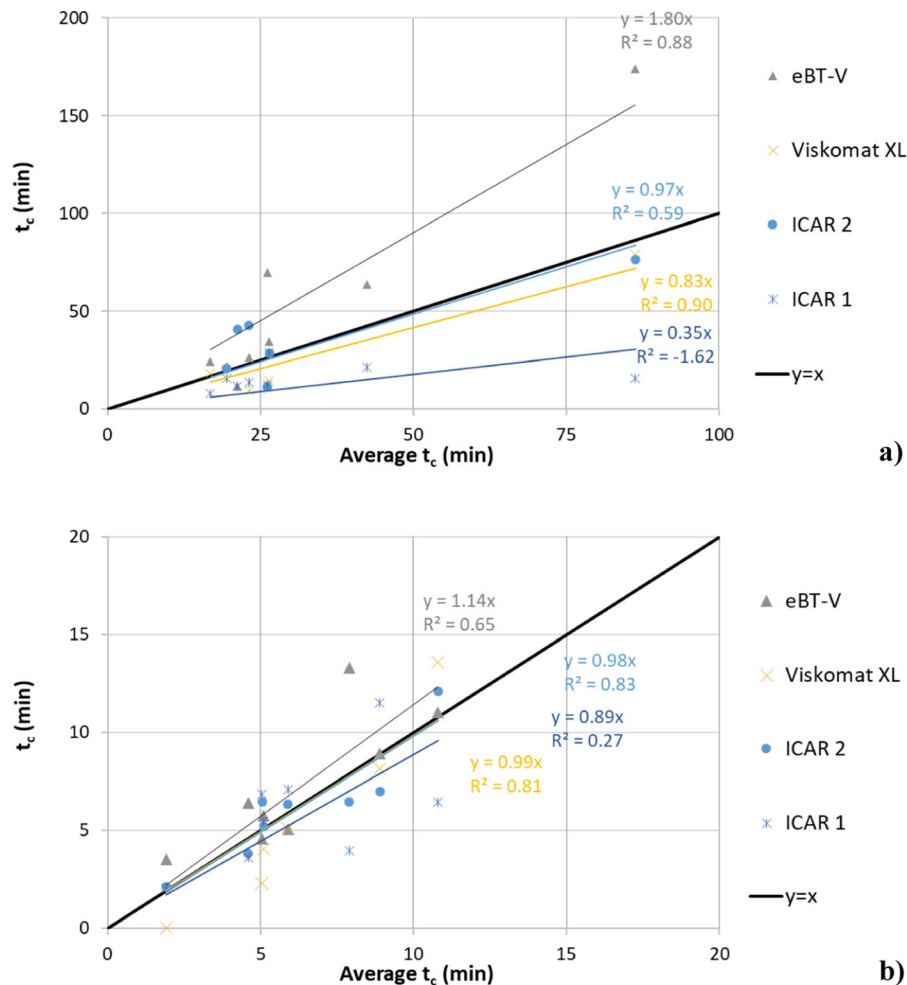


Fig. 7 Measured t_c obtained with (a) static yield stress measurements at 10 and 40 min (two values) vs. average t_c values computed for each tested material, and (b) static yield

stress measurements at 10 and 40 min and dynamic yield stress (three values) in vs. average t_c values computed for each tested material

mixtures because of the granular friction effect and the shear-induced particle migration.

It is interesting to note that the ranking between t_c values obtained for each rheometer compared using the slopes of the different regression lines is different than for A_{thix} . Comparing Figs. 4, 5, 6, 7, it is shown that the ranking of the rheometers completely changes between A_{thix} and t_c . Indeed, the ratio used in the computation of t_c deletes the effect of the initial calibration of the torque sensor of the rheometer and deletes the calibration-induced ranking. The various fitting parameters reported in Figs. 7 and computed from data are summarized in Table 1.

4.4 $\tau_{0,s10} \cdot A_{thix}$ thixotropic index

In order to compare all data obtained from the round-robin test campaign, the coupled-effect index values were plotted versus the average values of the coupled-effect index for each tested material. The average values were computed using test results obtained with the different rheometers for the same mixture. Data were analyzed using the coupled-effect index derived from the static yield stress measurements carried out after 10 and 40 min (Fig. 8a) and from the static yield stress measurements carried out after 10 and 40 min and the dynamic yield stress value (Fig. 8b). Again, the plate test was not considered because the initial

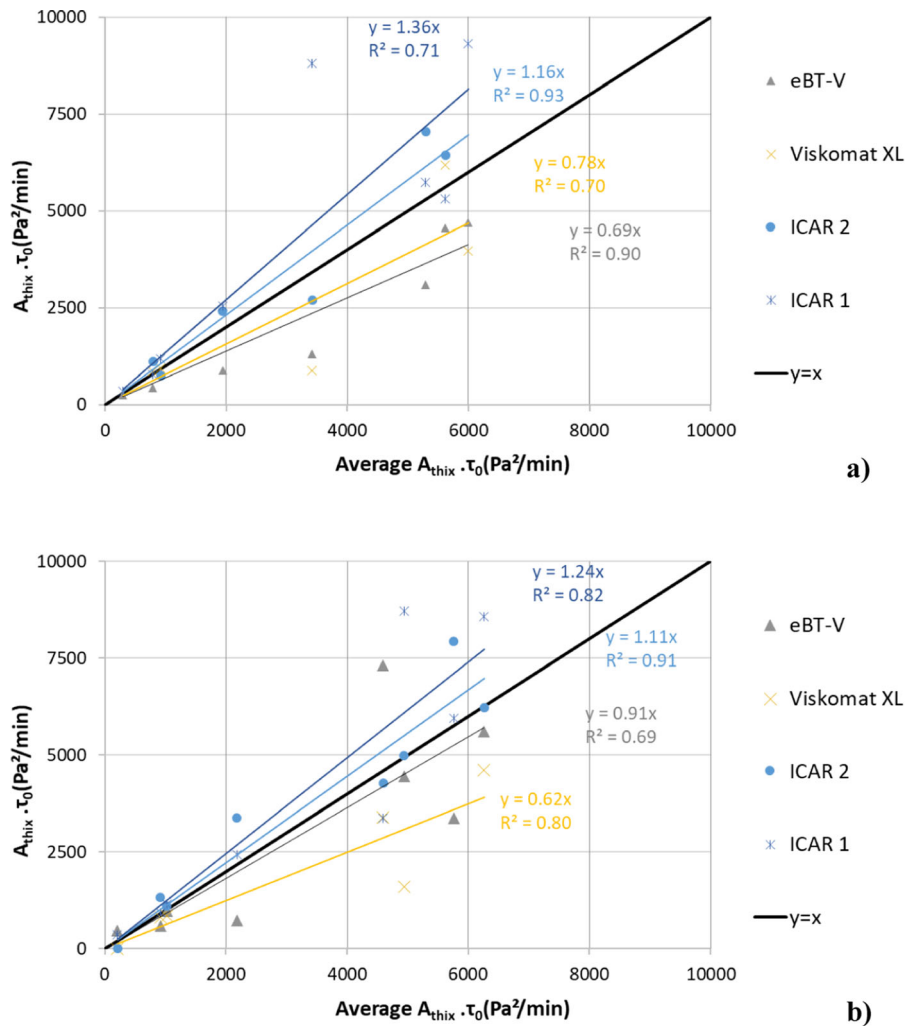


Fig. 8 Measured coupled effect indices obtained with (a) static yield stress measurements at 10 and 40 min (two values) vs. average coupled effect indices computed for each tested

material, and (b) static yield stress measurements at 10 and 40 min and dynamic yield stress (three values) vs. average coupled effect index values computed for each tested material

yield stress was not measured using the plate test device.

In Fig. 8a, it can be seen that all coupled-effect index values were dispersed around the computed average values for each mixture. The comparison of the linear fit parameter shows that the ICAR 1 rheometer provided the highest coupled-effect index (coefficient equal to 1.36), and the eBT-V rheometer provided the lowest coupled-effect index (coefficient equal to 0.69). The ranking of rheometers was the same as the one obtained with the A_{thix} . Other devices provided values that are close to the average line (0.78 for the Viskomat

XL rheometer and 1.16 for the ICAR 2 rheometer) with R^2 values ranging between 0.7 and 0.93.

The comparison of Fig. 8a and b shows that the computation of values with three yield stress values instead of two values allowed to noticeably reduce the dispersion of the measured critical time. Using a the two-point computation approach led to a linear fit coefficient ranging from 0.69 to 1.36, while the three-point approach reduced this range between 0.62 to 1.24. The R^2 coefficient for each rheometer was almost the same when using the three yield stress values.

It is interesting to distinguish measurement carried out on mortar for the 2- and 3-point computations and on concrete for the 2 and 3-points computations by analysing the data presented in Table 1. Contrary to the previous analysis, it can be seen that for both types of material (i.e., mortar and concrete), using three values of yield stress does not help to reduce the dispersion of the measurements. For the mortar mixtures, the linear fit coefficients ranged between 0.8 and 1.15 with the yield stress values measured at 10 and 40 min, and these values varied from 0.74 to 1.56 when the dynamic yield stress value was considered. For the concrete, the trend was the same, but the coupled-effect index values were more dispersed, as shown by the linear fit coefficients (0.57–1.52 using the 2-point computational approach and 0.58–1.34 using the 3-point computational approach). It is also worth noting that the mortars provided higher R^2 values close to 1 (between 0.97 and 0.99 with the 3-point computational approach) compared to those of 0.65 and 0.88 for the concrete mixtures tested with the rotational rheometers. The various fitting parameters reported in Figs. 8 and computed from data are summarized in Table 1.

4.5 Discussions on data analysis

The data analysis of the experimental results shows that the three tested structural build-up indices can provide similar information. The dispersion around the various average values of the indices was quite similar, even if the critical time t_c noticeably showed closer values between the various rheometers, as discussed in Sect. 4.3. The fact that this index allows to discard the difference in torque sensor calibration between rheometers can be a real advantage to compare values obtained from different rheometers.

It is interesting to note that the increase in the number of yield stress values (here from two to three data points) to determine the various indices can reduce the dispersion between the various indices. Therefore, the use of only two measurement values of static yield stress is not sufficient to secure accurate determination of the structural build-up of mortar and concrete.

In comparison with the round-robin testing campaign, the use of the single batch approach appears to be a promising solution to obtain more yield stress values. This single-batch approach validated at the

mortar scale [42] should be verified for concrete mixtures in further work.

5 Conclusions

The benchmark used to analyse the three thixotropy indices of the three mortar and five concrete mixtures designed with different yield stress and viscosity levels that were investigated in this study led to the following conclusions:

- The three thixotropy indices (yield stress variation with time, characteristic time, coupled effect) indicated the same thixotropic trend for the mortars and concretes, whether with the static method (plate test) or with the rheometric tests (ICAR, Viscomat XL, and eBT-V rheometers).
- The index values showed a good correlation for mortar mixtures. The thixotropy indices were, on the contrary, much more dispersed for the concrete mixtures.
- The quality of the correlations increased drastically as soon as the number of yield stress values used in the analysis increased from two to three measuring points, except for the coupled effect indices.
- The static plate test method and rheometric methods can be adapted to evaluate the structural build-up of mortar mixtures so long that the static yield stress obtained with the stress growth method can be accurately measured immediately after the application of shear rate. Data sampling should be of the order of 1/100 of a second to ensure adequate capturing of peak torque values during shear growth testing.
- The plate test should be carried out carefully ensuring that the materials at the top of the tested samples (where the bar is placed) is not subjected to bleeding, and that the material does not slip at the plate interface.
- It is recommended to increase the number of yield stress values to at least four points over one hour after mixing to determine more accurately the various thixotropy indices. For example, t_0 , $t_0 + 5$, $t_0 + 15$, $t_0 + 30$, and $t_0 + 50$ min. The measurement points must be selected in the linear range of static yield stress growth; shorter testing duration should be selected though in highly



thixotropic mixtures when an exponential variation in static yield stress takes place at later ages.

- In order to reduce the dispersion of the thixotropy indices of concrete, the use of larger diameter rheometer containers is recommended to be more consistent with the maximum size of the coarse aggregate in the sheared material. This point should be the matter of a future work or benchmark. The use of a single batch approach appears to be a promising solution.

Acknowledgements The authors recognize the help of the scientific and technical team at the Université d'Artois, LGCgE Laboratoire de Génie Civil et Géo-Environnement. The authors are grateful to Mr. Faber Fabbris from concrete producer EQIOM for planning and providing “just in time” mortar and concrete mixtures of different rheological properties. The authors are very thankful to all other participants in the round-robin testing campaign: Geert De Schutter, Chafika Djelal, Khadija El Cheikh, Faber Fabbris, Shirin Fataei, Dimitri Feys, Markus Greim, Irina Ivanova, Laurent Libessart, Helena Keller, Viktor Mechtcherine, Ivan Navarrete, Egor Secrieru, Yannick Vanhove and their organisations.

Author's contribution This document is the result of an experimental campaign supported by and carried out by a task group of RILEM TC 266-MRP. Other members of the task group who contributed to the experimental campaign and data treatment are: DF, ES, HK, KE, YV, CD, SF, MG, II, LL, VM, and IN. Other members of RILEM TC 266-MRP, not involved in the task group are: RC, GDS, SF, SG, MH, SJ, KL, JL, DL, TP, NR, WS, JV, JEW, AY, and JZ. This paper was reviewed and approved by all members of the committee.

Declarations

Conflict of interest None of the authors declare a conflict of interest.

References

- Roussel N (2006) A thixotropy model for fresh fluid concretes: theory, validation and applications. *Cem Concr Res* 36:1797–1806. <https://doi.org/10.1016/j.cemconres.2006.05.025>
- Roussel N, Lemaître A, Flatt RJ, Coussot P (2010) Steady state flow of cement suspensions: a micromechanical state of the art. *Cem Concr Res* 40:77–84. <https://doi.org/10.1016/j.cemconres.2009.08.026>
- Wallevik JE (2009) Rheological properties of cement paste: thixotropic behavior and structural breakdown. *Cem Concr Res* 39:14–29. <https://doi.org/10.1016/j.cemconres.2008.10.001>
- Wallevik JE, Rheocenter I, Iceland IC (2011) Particle flow interaction theory-thixotropic behavior and structural breakdown. In: Proceedings of the Conference on Our World of Concrete and Structures, Singapore. pp 14–16
- Assaad J, Khayat KH, Mesbah H (2003) Assessment of thixotropy of flowable and self-consolidating concrete. *Mater J* 100:99–107
- Roussel N (2005) Steady and transient flow behaviour of fresh cement pastes. *Cem Concr Res* 35:1656–1664. <https://doi.org/10.1016/j.cemconres.2004.08.001>
- Lecompte T, Perrot A (2017) Non-linear modeling of yield stress increase due to SCC structural build-up at rest. *Cem Concr Res* 92:92–97. <https://doi.org/10.1016/j.cemconres.2016.11.020>
- Perrot A, Pierre A, Vitaloni S, Picandet V (2015) Prediction of lateral form pressure exerted by concrete at low casting rates. *Mater Struct* 48:2315–2322. <https://doi.org/10.1617/s11527-014-0313-8>
- Ma S, Qian Y, Kawashima S (2018) Experimental and modeling study on the non-linear structural build-up of fresh cement pastes incorporating viscosity modifying admixtures. *Cem Concr Res* 108:1–9
- Kruger J, Zeranka S, van Zijl G (2019) 3D concrete printing: a lower bound analytical model for buildability performance quantification. *Autom Constr* 106:102904. <https://doi.org/10.1016/j.autcon.2019.102904>
- Roussel N (2018) Rheological requirements for printable concretes. *Cem Concr Res* 112:76–85. <https://doi.org/10.1016/j.cemconres.2018.04.005>
- Perrot A, Rangeard D, Pierre A (2016) Structural built-up of cement-based materials used for 3D-printing extrusion techniques. *Mater Struct* 49:1213–1220. <https://doi.org/10.1617/s11527-015-0571-0>
- Roussel N, Ovarlez G, Garrault S, Brumaud C (2012) The origins of thixotropy of fresh cement pastes. *Cem Concr Res* 42:148–157. <https://doi.org/10.1016/j.cemconres.2011.09.004>
- Omran AF, Naji S, Khayat KH (2011) Portable vane test to assess structural buildup at rest of self-consolidating concrete. *ACI Mater J* 108:628–637
- Lecompte T, Perrot A, Picandet V et al (2012) Cement-based mixes: shearing properties and pore pressure. *Cem Concr Res* 42:139–147
- Assaad J, Khayat KH (2004) Influence of internal friction and cohesion on the variations of formwork pressure of self-consolidating concrete. *Spec Publ* 222:19–32
- Feys D, Sonebi M, Amziane S, et al RILEM TC 266-MRP - Round-Robin rheological tests on high performance mortar and concrete with adapted rheology: rheometers, mixtures and procedures. *Mater Struct* 56(4):90
- Lapasin R, Papo A, Rajgelj S (1983) Flow behavior of fresh cement pastes. A comparison of different rheological instruments and techniques. *Cem Concr Res* 13:349–356
- Mantellato S, Palacios M, Flatt RJ (2019) Relating early hydration, specific surface and flow loss of cement pastes. *Mater Struct* 52:5. <https://doi.org/10.1617/s11527-018-1304-y>
- Khayat KH, Omran AF, Naji S et al (2012) Field-oriented test methods to evaluate structural build-up at rest of flowable mortar and concrete. *Mater Struct* 45:1547–1564. <https://doi.org/10.1617/s11527-012-9856-8>
- Megid WA, Khayat KH (2018) Evaluating structural buildup at rest of self-consolidating concrete using workability tests. *ACI Mater J* 115:257–265



22. Ovarlez G, Roussel N (2006) A physical model for the prediction of lateral stress exerted by self-compacting concrete on formwork. *Mater Struct* 39:269–279. <https://doi.org/10.1617/s11527-005-9052-1>
23. Perrot A, Amziane S, Ovarlez G, Roussel N (2009) SCC formwork pressure: influence of steel rebars. *Cem Concr Res* 39:524–528
24. Assaad JJ, Khayat KH (2006) Effect of casting rate and concrete temperature on formwork pressure of self-consolidating concrete. *Mater Struct* 39:333–341
25. Billberg PH, Roussel N, Amziane S et al (2014) Field validation of models for predicting lateral form pressure exerted by SCC. *Cement Concr Compos* 54:70–79
26. Khayat K, Assaad J, Mesbah H, Lessard M (2005) Effect of section width and casting rate on variations of formwork pressure of self-consolidating concrete. *Mater Struct* 38:73–78
27. Gardner NJ, Keller L, Khayat KH et al (2016) Field measurements of SCC lateral pressure—Toronto 2014. *Lateral* 12:14
28. Saric-Coric M, Khayat KH, Tagnit-Hamou A (2003) Performance characteristics of cement grouts made with various combinations of high-range water reducer and cellulose-based viscosity modifier. *Cem Concr Res* 33:1999–2008
29. Naji S, Khayat KH, Karray M (2017) Assessment of static stability of concrete using shear wave velocity approach. *ACI Mater J* 114:105–115
30. Roussel N, Cussigh F (2008) Distinct-layer casting of SCC: the mechanical consequences of thixotropy. *Cem Concr Res* 38:624–632. <https://doi.org/10.1016/j.cemconres.2007.09.023>
31. Megid WA, Khayat KH (2017) Bond strength in multilayer casting of self-consolidating concrete. *ACI Mater J* 114:467–476
32. Megid WA, Khayat KH (2019) Effect of structural buildup at rest of self-consolidating concrete on mechanical and transport properties of multilayer casting. *Constr Build Mater* 196:626–636
33. Shahab AR, Lloret Kristensen E, Fischer P, et al (2013) Smart dynamic casting or how to exploit the liquid to solid transition in cementitious materials. In: 7th RILEM International Conference on Self-Compacting Concrete and 1st RILEM International Conference on Rheology and Processing of Construction Materials
34. Wolfs RJM, Bos FP, Salet TAM (2018) Early age mechanical behaviour of 3D printed concrete: numerical modelling and experimental testing. *Cem Concr Res* 106:103–116. <https://doi.org/10.1016/j.cemconres.2018.02.001>
35. Mechtcherine V, Bos FP, Perrot A et al (2020) Extrusion-based additive manufacturing with cement-based materials – production steps, processes, and their underlying physics: a review. *Cement Concr Res* 132:106037. <https://doi.org/10.1016/j.cemconres.2020.106037>
36. Reiter L, Wangler T, Roussel N, Flatt RJ (2018) The role of early age structural build-up in digital fabrication with concrete. *Cem Concr Res* 112:86–95. <https://doi.org/10.1016/j.cemconres.2018.05.011>
37. Perrot A, Lecompte T, Estellé P, Amziane S (2013) Structural build-up of rigid fiber reinforced cement-based materials. *Mater Struct* 46:1561–1568
38. Amziane S, Perrot A (2017) The plate test carried out on fresh cement-based materials: How and why? *Cem Concr Res* 93:1–7. <https://doi.org/10.1016/j.cemconres.2016.12.002>
39. Lootens D, Jousset P, Martinie L et al (2009) Yield stress during setting of cement pastes from penetration tests. *Cem Concr Res* 39:401–408. <https://doi.org/10.1016/j.cemconres.2009.01.012>
40. Ivanova I, Mechtcherine V (2019) Evaluation of structural build-up rate of cementitious materials by means of constant shear rate test: parameter study. In: *Rheology and Processing of Construction Materials*. Springer, pp 209–218
41. Ivanova I, Mechtcherine V (2020) Possibilities and challenges of constant shear rate test for evaluation of structural build-up rate of cementitious materials. *Cem Concr Res* 130:105974
42. Ivanova I, Mechtcherine V (2020) Effects of volume fraction and surface area of aggregates on the static yield stress and structural build-up of fresh concrete. *Materials* 13:1551
43. Nerella VN, Beigh MAB, Fataei S, Mechtcherine V (2019) Strain-based approach for measuring structural build-up of cement pastes in the context of digital construction. *Cem Concr Res* 115:530–544. <https://doi.org/10.1016/j.cemconres.2018.08.003>
44. Feys D, Wallevik JE, Yahia A et al (2012) Extension of the Reiner-Riwlin equation to determine modified Bingham parameters measured in coaxial cylinders rheometers. *Mater Struct* 46:289–311. <https://doi.org/10.1617/s11527-012-9902-6>
45. Wallevik OH, Feys D, Wallevik JE, Khayat KH (2015) Avoiding inaccurate interpretations of rheological measurements for cement-based materials. *Cem Concr Res* 78:100–109
46. Yuan Q, Zhou D, Khayat KH et al (2017) On the measurement of evolution of structural build-up of cement paste with time by static yield stress test vs. small amplitude oscillatory shear test. *Cem Concr Res* 99:183–189
47. Teng L, Zhu J, Khayat KH, Liu J (2020) Effect of welan gum and nanoclay on thixotropy of UHPC. *Cem Concr Res* 138:106238
48. Dzuy NQ, Boger DV (1985) Direct yield stress measurement with the vane method. *J Rheol* 29:335–347
49. Mahaut F, Mokéddem S, Chateau X et al (2008) Effect of coarse particle volume fraction on the yield stress and thixotropy of cementitious materials. *Cem Concr Res* 38:1276–1285. <https://doi.org/10.1016/j.cemconres.2008.06.001>
50. Khalil N, Aouad G, El Cheikh K, Rémond S (2017) Use of calcium sulfoaluminate cements for setting control of 3D-printing mortars. *Constr Build Mater* 157:382–391
51. Stokes J, Telford J (2004) Measuring the yield behaviour of structured fluids. *J Nonnewton Fluid Mech* 124:137–146. <https://doi.org/10.1016/j.jnnfm.2004.09.001>
52. Feys D, Cepuritis R, Jacobsen S et al (2018) Measuring rheological properties of cement pastes: most common techniques, procedures and challenges. *RILEM Tech Lett* 2:129–135
53. Qian Y, Kawashima S (2018) Distinguishing dynamic and static yield stress of fresh cement mortars through thixotropy. *Cement Concr Compos* 86:288–296



54. Qian Y, Kawashima S (2016) Use of creep recovery protocol to measure static yield stress and structural rebuilding of fresh cement pastes. *Cem Concr Res* 90:73–79
55. Ferraris CF, Brower LE, Banfill PFG (2001) NISTIR 6819: Comparison of concrete rheometers: International tests at LCPC (Nantes, France) in October, 2000. US Department of Commerce, National Institute of Standards and Technology
56. Ferraris CF, Ferraris CF, Beaupr D, et al (2004) Comparison of concrete rheometers: International tests at MB (Cleveland OH, USA) in May, 2003. US Department of Commerce, National Institute of Standards and Technology
57. Koehler EP (2004) Development of a portable rheometer for Portland cement concrete. Master of Sciences Thesis, University of Texas, Austin
58. Feys D, Keller H, El Cheikh K, et al RILEM TC 266-MRP: Round-Robin rheological tests on high performance mortar and concrete with adapted rheology: a comprehensive flow curve analysis. *Mater Struct* 56(5):105
59. Sleiman H, Perrot A, Amziane S (2010) A new look at the measurement of cementitious paste setting by Vicat test. *Cem Concr Res* 40:681–686. <https://doi.org/10.1016/j.cemconres.2009.12.001>
60. Tchamba JC, Amziane S, Ovarlez G, Roussel N (2008) Lateral stress exerted by fresh cement paste on formwork: laboratory experiments. *Cem Concr Res* 38:459–466. <https://doi.org/10.1016/j.cemconres.2007.11.013>
61. Amziane S, Perrot A, Lecompte T (2008) A novel settling and structural build-up measurement method. *Meas Sci Technol* 19:105702
62. Zhang M-H, Ferraris C, Zhu H et al (2010) Measurement of yield stress for concentrated suspensions using a plate device. *Mater Struct* 43:47–62. <https://doi.org/10.1617/s11527-009-9469-z>
63. Svermova L, Sonebi M, Bartos PJ (2003) Influence of mix proportions on rheology of cement grouts containing limestone powder. *Cement Concr Compos* 25:737–749
64. Coussot P, Boyer S (1995) Determination of yield stress fluid behaviour from inclined plane test. *Rheol Acta* 34:534–543

Publisher's Note Springer Nature remains neutral with regard to jurisdictional claims in published maps and institutional affiliations.

Springer Nature or its licensor (e.g. a society or other partner) holds exclusive rights to this article under a publishing agreement with the author(s) or other rightsholder(s); author self-archiving of the accepted manuscript version of this article is solely governed by the terms of such publishing agreement and applicable law.

